Optik 154 (2018) 510–515

Contents lists available at ScienceDirect

Optik

journal homepage: www.elsevier.de/ijleo

Full length article

Fabrication and characterization of rutile-phased titanium dioxide (TiO_2) nanorods array with various reaction times using one step hydrothermal method

S.M. Mokhtar[a], M.K. Ahmad[a,*], C.F. Soon[a], N. Nafarizal[a], A.B. Faridah[b], A.B. Suriani[c], M.H. Mamat[d], M. Shimomura[e], K. Murakami[e]

[a] *Microelectronic and Nanotechnology – Shamsuddin Research Centre (MiNT-SRC), Faculty of Electrical and Electronic Engineering, Universiti Tun Hussein Onn Malaysia, 86400 Parit Raja, Batu Pahat, Johor, Malaysia*
[b] *Department of Science, Faculty of Science, Technology, and Human Development, Universiti Tun Hussein Onn Malaysia, 86400 Parit Raja, Batu Pahat, Johor, Malaysia*
[c] *Nanotechnology Research Centre, Department of Physic, Faculty of Science and Mathematics, Universiti Pendidikan Sultan Idris, 35900 Tanjung Malim, Perak, Malaysia*
[d] *Nano-ElecTronic Centre, Faculty of Electrical Engineering, UiTM, 40450 Shah Alam, Selangor, Malaysia*
[e] *Department of Engineering, Graduate School of Integrated Science and Technology, Shizuoka University, 432-8011 Hamamatsu, Shizuoka, Japan*

ARTICLE INFO

Article history:
Received 25 July 2017
Accepted 18 October 2017

Keywords:
TiO_2
Nanorods array
One-step hydrothermal method
Raman

ABSTRACT

Rutile titanium dioxide nanorods array were fabricated on fluorine-doped tin oxide by using hydrothermal method. The influences of hydrothermal reaction time on morphology, structure property, crystallization, and Raman spectra have been investigated. The hydrothermal treatment was conducted by varying the reaction time at 4, 10, 16, and 24 h with temperature of 150 °C. The nanostructure samples were analyzed using field emission-scanning electron microscope, X-ray diffractometer, and micro-Raman spectroscopy. The resulting nanorods array shows increasing diameter as the reaction time increased. Meanwhile, the growth of the nanorods stop at one point as can be seen in its thickness, x-ray diffraction, and Raman spectra. This behavior can be attributed to hydrolysis rate of the precursor titanium butoxide (TBOT) as the reaction time increased.

1. Introduction

Titanium dioxide (TiO_2) exists in three known crystalline that is anatase, rutile, and brookite with polymorphs tetragonal for both anatase and rutile, and orthorhombic for brookite [1]. TiO_2 have received significant notice these past few decades after the discoveries of photoelectrochemical cell (PEC) and dye sensitized solar cell [2,3]. Major drawbacks of TiO_2 nanoparticles related to its recombination process during cell performance [4]. To overcome the drawback, TiO_2 nanostructures such as nanorods, nanoflowers, and nanowires were introduced, as its exhibit excellent electron transport due to its well-defined crystalline structure and unique optical properties, which minimizes the recombination process and have been considered as a substitute in the solar cells and electronic devices [5–11]. As TiO_2 nanostructures exhibit high crystallinity properties, the electron mobility is also high, thus indirectly enhanced the electron transport and minimize the recombination losses in the thin film [12–14]. There are several methods to produces these nanostructures such as sol-gel, chemical bath deposition

* Corresponding author.
E-mail address: akhairul@uthm.edu.my (M.K. Ahmad).

https://doi.org/10.1016/j.ijleo.2017.10.091
0030-4026/

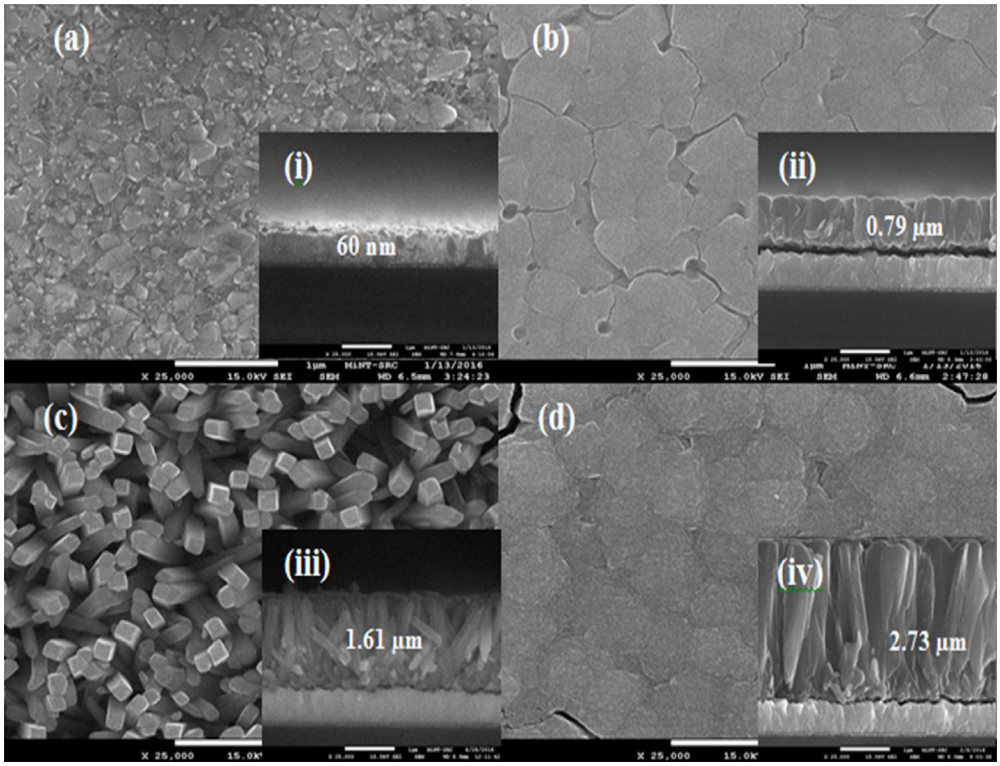

Fig. 1. Surface morphology of TiO_2 nanorods array fabricated with different hydrothermal reaction times from (a) 4, (b) 10, (c) 16, and (d) 24 h, cross-sectional images of (i) 4, (ii) 10, (iii) 16 and (iv) 24 h hydrothermal reaction time.

(CBD), chemical vapor deposition (CVD), and hydrothermal method. In this study, TiO_2 was fabricated by using hydrothermal method. Other methods were at disadvantages such as CBD and CVD methods that usually use an elevated temperature around 300–400 °C, while for sol-gel, there is often a cracking and large volume shrinkage during drying process [15–19]. Hydrothermal synthesis method uses a low temperature for mass production of well aligned TiO_2 nanostructures directly on substrates, which in this study are using a fluorine-doped tin oxide (FTO) substrate. By using FTO, the preparation for seed layer can be eliminated. In this study, the thin film TiO_2 fabricated were in rutile-phase. Highly crystalline TiO_2 were intensively investigated due to its advantages such as easily controllable diameter and thickness [20], as well as high electron mobility and chemical stability [21,22] compared to anatase and brookite. These features make it suitable for applications such as photocatalyst and ultraviolet photodetector [23,24].

2. Experimental

Titanium dioxide nanorods array were synthesized using the hydrothermal process in a chemical solution. 120 mL of concentrated hydrochloric acid was dissolved in 120 mL of deionized (DI) water. After vigorously stirred for 5 min, 3.5 mL of titanium butoxide (TBOT) was added dropwise using capillary tube. After that, the solution was poured into the autoclave with Teflon-made liner for hydrothermal process to begin. Hydrothermal reaction takes place at 150 °C with reaction times of 4, 10, 16 and 24 h. After that, the autoclave was taken out from the oven and was let to cool to room temperature. The sampe was then rinsed with DI water and left to dry in oven with 60 °C for 10 min. Field emission scanning electron microscope (FESEM) JEOL JSM-7600F model operated at 15 kV was used to characterize the morphology and thickness of the samples. Meanwhile, the crystal structure and crystallite size are defined by an X-ray diffractometer (XRD) PANalytical X-Pert3 Powder model. The scan axis used was 2 h with range of $20\theta - 60\theta$ and the type of slit used were fixed divergence slit. Finally, Raman spectra were obtained using a Micro-Raman Spectroscope (Renishaw InVia microRaman System) operated with 514 nm wavelength of argon (Ar^+) laser.

3. Results and discussion

3.1. Field-emission scanning electron microscopy

Fig. 1 shows the FESEM image of the nanorods array grown on top of the FTO layer at different reaction times ranging from 4 h to 24 h. Fig. 1(a)–(d) showed the surface of the nanorods with reaction times of 4 h, 10 h, 16 h, and 24 h, respectively. It

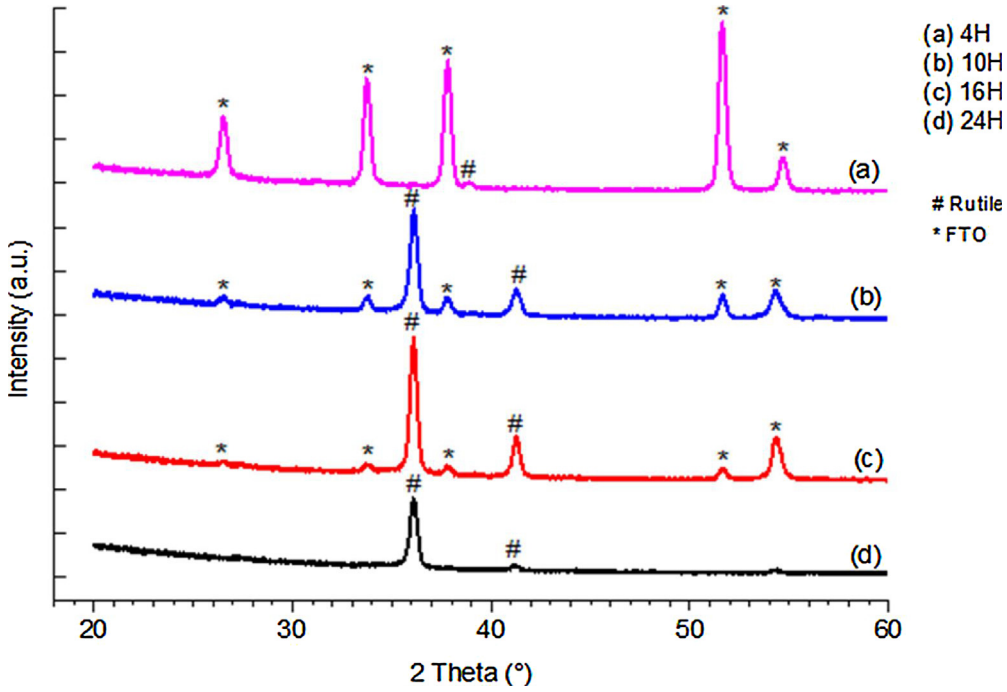

Fig. 2. XRD patterns of TiO_2 nanorods array fabricated with different hydrothermal reaction time from (a) 4, (b) 10, (c) 16, and (d) 24 h.

can be clearly seen that the nanorods grew in decent shape after the reaction time of 16 h. Fig. 1(a) shows that the nanorods can barely be seen as the reaction time was too short for growth of the nanorods with diameter produced ranging from 30 to 45 nm. The rods are in slanting position with large gaps between each other. However, the nanorods started to grow with increasing reaction time, as can be observed in Fig. 1(b) and (c), with size ranges from 250 to 450 nm and 250–300 nm, respectively. It can be seen on the surface structure of Fig. 1(b) that the nanorods started to develop in tetragonal shape and a gap between the nanorods has started to form. Meanwhile, from Fig. 1(c), it can be seen that the TiO_2 nanorods have grown in decent tetragonal shape with a flat-end facets and obvious gap between them. As the reaction time further increase, the nanorods agglomerate to each other, thus eliminating the gap between the nanorods and the rods also lose their tetragonal forms resulting diameter ranges from 200 to 450 nm as shown in Fig. 1(d). A cross-sectional image of the synthesized TiO_2 nanorods array is shown in Fig. 1(i), (ii), (iii), and (iv) for 4, 10, 16, and 24 h reaction time, respectively. For Fig. 1(i), the cross sectional image shows only of FTO substrate as the nanorods were too small and almost invisible as can be seen in Fig. 1(a). Overall image shows that the nanorods grew perpendicular to the substrate with length of the nanorods to be 0.79 μm for Fig. 1(ii), 1.61 μm for Fig. 1(iii), and 2.73 for Fig. 1(iv). It can be concluded that the lengths of TiO_2 nanorods increase with increasing reaction time [1].

3.2. X-ray diffraction

The XRD patterns of the nanorods TiO_2 prepared with different reaction times are shown in Fig. 2(a)–(d) for 4 h, 10 h, 16 h and 24 h, respectively. Clear diffraction peaks are recorded between 20° and 60° consisting of rutile TiO_2 and FTO peaks. The rutile peaks are indexed to (101), (200), and (111) planes of TiO_2 with tetragonal structures. Fig. 2(a) shows dominant peaks of FTO at 26°, 34°, 37°, 51°, 55° and a rutile TiO_2 peak at 39° of plane (200). This is confirmed with FESEM image which shows mostly FTO surface and nanorods only starting to grow on it. XRD diffraction for nanorods prepared in 10 and 16 h reaction times as shown in Fig. 2(b) and (c), respectively, were a mixed of FTO and rutile peaks. Both samples prepared have two rutile peaks correspond to planes (101) and (111) with insignificant change in their intensity. In the meantime, intensity for FTO peaks have decreased due to the thickness of the thin film that increased with increasing time as stated in FESEM analysis. In Fig. 2(d), it can be seen that there is no FTO peaks produced leaving only rutile TiO_2 peaks as the diffraction with a slight drop in its intensity. Fig. 2 shows that the (101) plane orientation peak centred at 36° gave the highest intensity for rutile TiO_2 compared to the others. This indicates that the nanorods growth occurred preferentially vertically to the FTO substrate. Overall peaks observed gave either a strong, sharp diffraction, or a weak, sharp diffraction. There is no broad peak produced thus showing good crystallinity of the samples. During the growth of TiO_2 nanorods on FTO substrates, the SnO_2 act as a nucleation layer. In order to reduce the surface energy by terminating high energy facets, attachment always takes place at the high energy surfaces. As both rutile and SnO_2 have tetragonal structure where the surface energy of (101) plane is high, growth of titania crystal occurs instantly. While the thermodynamically stable crystal structure of SnO_2 is rutile, the

Table 1
Full-width Half-Maximum and crystallite size of sample fabricated with different reaction time.

Reaction time (hour)	Full-Width Half-Maximum (FWHM)	Crystallite Size (Å)
4	0.393	242.4
10	0.315	307.93
16	0.138	770.2
24	0.138	770.2

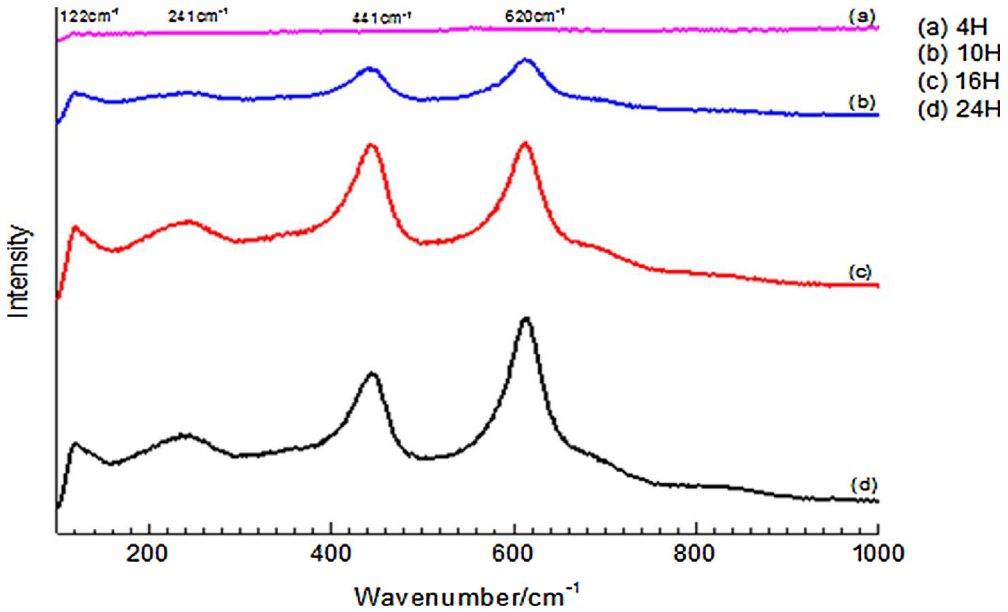

Fig. 3. Raman spectra of TiO_2 nanorods array fabricated with different hydrothermal reaction times from (a) 4, (b) 10, (c) 16, and (d) 24 h.

very small lattice mismatch of both TiO_2 and FTO substrate were the driving force for the epitaxial growth of TiO_2 nanorod arrays [25]. Table 1 shows the obtained crystallite size for each sample. Different reaction times gave quite a significant change in the crystallite size, except for 16 and 24 h reaction time where the crystallite sizes are the same. The crystallite size increases when time increases as increasing time allowing greater coalescence of the particles [26,27].

3.3. *Raman spectroscopy*

Raman spectra of TiO_2 nanorods with different reaction times are shown in Fig. 3(a)–(d) for 24 h, 16 h, 10 h and 4 h, respectively. Peak position produced for Fig. 3(a) are normalized as shown in Fig. 4, which shows only the peaks of FTO at 570 cm^{-1} and 1087 cm^{-1}. Starting from Fig. 3(b) to (c), all peaks produced are of rutile TiO_2 Raman shifts at 122 cm^{-1}, 241 cm^{-1}, 441 cm^{-1}, and 620 cm^{-1} which confirmed the result of XRD peaks. Three of the peaks, 122 cm^{-1}, 441 cm^{-1}, and 620 cm^{-1} are the dominant peaks of rutile single crystal expressed as $A_{1g} + B_{1g} + E_g$. There is also a second-order scattering peak at 241 cm^{-1} which is also a characteristic of rutile TiO_2. The weak and broad peak produced at 241 cm^{-1} was likely because of phonon confinement effect [1]. The samples show increasing intensity of the Raman peaks with increasing reaction time at its prominent maxima which are at 441 cm^{-1} and 620 cm^{-1}. This indicated that the nanorods prepared with longer reaction time have better crystallinity as had been in agreement with XRD patterns shown in Fig. 2. This result also suggests that thickness of the sample increase with increasing reaction time.

4. Conclusions

Titanium dioxide thin films have been successfully fabricated on top fluorine-doped tin oxide by using hydrothermal method. The reaction time was varied from 4 to 24 h. FESEM image of the resulting thin films shows that the diameter of the nanorods increased with increasing reaction time, and the crystalline structure shows rutile phase in all sample fabricated according to XRD pattern and Raman spectra.

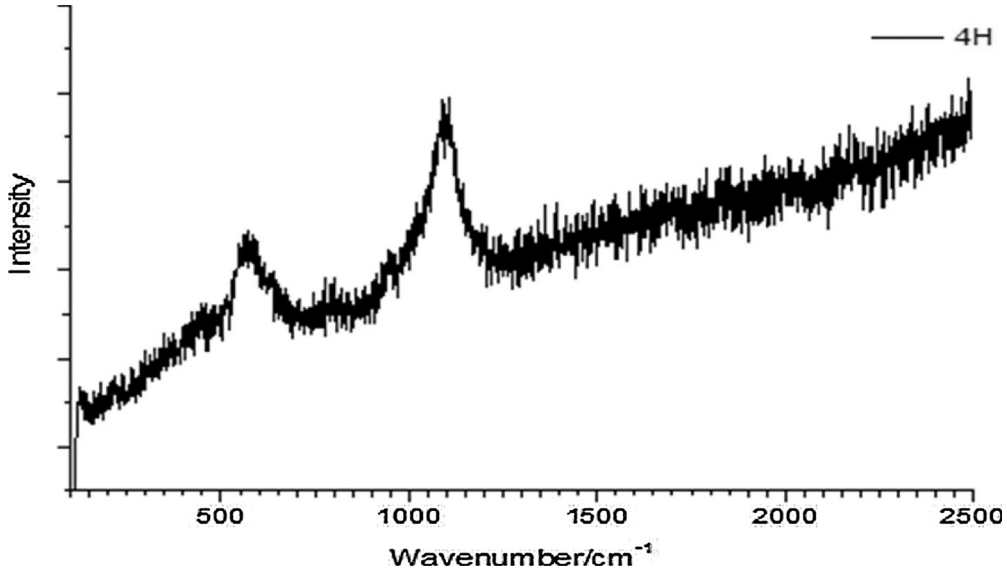

Fig. 4. Normalized Raman spectra of TiO_2 nanorods array fabricated with 4 h hydrothermal reaction time.

Acknowledgements

The authors would like to thank the Ministry of Education (MOE) Malaysia, Microelectronic and Nanotechnology-Shamsuddin Research Centre (MiNT-SRC) and Universiti Tun Hussein Onn Malaysia (UTHM) for financial support using Vot STG U347.

References

[1] M.K. Ahmad, S.M. Mokhtar, C.F. Soon, N. Nafarizal, A.B. Suriani, A. Mohamed, M.H. Mamat, M.F. Malek, M. Shimomura, K. Murakami, Raman investigation of rutile-phased TiO2 nanorods/nanoflowers with various reaction times using one step hydrothermal method, J. Mater. Sci. Mater. Electron. 27 (8) (2016) 7920–7926.
[2] A. Fujishima, K. Honda, © 1972 nature publishing group, Nature 238 (1972) 37–38.
[3] B. O'Regan, M. Gratzel, © 19 9 1 nature publishing group, Lett. Nat. 353 (1991) 737–740.
[4] P. Soundarrajan, K. Sankarasubramanian, T. Logu, K. Sethuraman, K. Ramamurthi, Growth of rutile Ti nanorods on TiO2 seed layer prepared using facile low cost chemical methods, Mater. Lett. 116 (February) (2014) 191–194.
[5] L. Lv, Q. Lu, Y. Ning, Z. Lu, X. Wang, Z. Lou, A. Tang, Y. Hu, F. Teng, Y. Yin, Y. Hou, Self-assembled TiO2 nanorods as electron extraction layer for high-performance inverted polymer solar cells, Chem. Mater. 27 (1) (2015) 44–52.
[6] V. Manthina, J. Pablo, C. Baena, G. Liu, A.G. Agrios, ZnO – TiO2 Nanocomposite Films for High Light Harvesting E Ffi Ciency and Fast Electron Transport in Dye-Sensitized Solar Cells, 2012.
[7] X. Li, C. Gao, H. Duan, B. Lu, Y. Wang, L. Chen, Z. Zhang, X. Pan, E. Xie, High-performance photoelectrochemical-type self-powered UV photodetector using epitaxial TiO2/SnO2 branched heterojunction nanostructure, Small 9 (11) (2013) 2005–2011.
[8] C. Li, C. Koenigsmann, W. Ding, B. Rudshteyn, K.R. Yang, K.P. Regan, S.J. Konezny, V.S. Batista, G.W. Brudvig, C.A. Schmuttenmaer, J.-H. Kim, Facet-dependent photoelectrochemical performance of TiO2 nanostructures: an experimental and computational study, J. Am. Chem. Soc. 137 (4) (2015) 1520–1529.
[9] S. Herná, D. Hidalgo, A. Sacco, A. Chiodoni, A. Lamberti, V. Cauda, E. Tresso, G. Saracco, Comparison of photocatalytic and transport properties of TiO2 and ZnO nanostructures for solar-driven water splitting, Phys. Chem. Chem. Phys. 17 (ii) (2015) 7775–7786.
[10] C. Wang, Z. Jiang, L. Wei, Y. Chen, J. Jiao, M. Eastman, H. Liu, Photosensitization of TiO2 nanorods with CdS quantum dots for photovoltaic applications: a wet-chemical approach, Nano Energy 1 (3) (2012) 440–447.
[11] X. Wang, X. Wang, H. Liu, W. Shen, Controllable in Situ Photo-assisted Chemical Deposition of CdSe Quantum Dots on ZnO / CdS Nanorod Arrays and Its Photovoltaic Application Controllable in Situ Photo-assisted Chemical Deposition of CdSe Quantum Dots on ZnO / CdS Nanorod Arrays and Its Phot, 2016, no August.
[12] Z. Sun, T. Liao, L. Sheng, L. Kou, J.H. Kim, S.X. Dou, Deliberate design of TiO2 nanostructures towards superior photovoltaic cells, Chem. - A Eur. J. (May) (2016) 11357–11364.
[13] N.M. Dimitrijevic, S. Tepavcevic, Y. Liu, in: Nada M. Dimitrijevic, Sanja Tepavcevic, Yuzi Liu (Eds.), 4. Nanostructured TiO2/polypyrrole for Visible Light Photocatalysis, 2015, pp. 2–7, no. January.
[14] E.J.W. Crossland, N. Noel, V. Sivaram, T. Leijtens, J.A. Alexander-Webber, H.J. Snaith, Mesoporous TiO2 single crystals delivering enhanced mobility and optoelectronic device performance, Nature 495 (7440) (2013) 215–219.
[15] I. Corporation, CVD Vs. PVD Advantages and Disadvantages 98752 R0, vol. 86, 2008, pp. 580400, 0.
[16] J.R. Creighton, P. Ho, Introduction to chemical vapor deposition (CVD) VA IVA, Chem. Vap. Depos. (2001) 11–13.
[17] O. Chemistry, Sols, Gels and Organic Chemistry, 2017, pp. 400–411.
[18] D. Hariskos, M. Powalla, N. Chevaldonnet, D. Lincot, A. Schindler, B. Dimmler, Chemical bath deposition of CdS buffer layer: prospects of increasing materials yield and reducing waste, Thin Solid Films 387 (1–2) (2001) 179–181.
[19] C. Fang, D. Zhang, S. Cai, L. Zhang, L. Huang, H. Li, P. Maitarad, L. Shi, R. Gao, J. Zhang, Low-temperature selective catalytic reduction of NO with NH(3) over nanoflaky MnOx on carbon nanotubes in situ prepared via a chemical bath deposition route, Nanoscale 5 (19) (2013) 9199–9207.
[20] Y. Liao, W. Que, Q. Jia, Y. He, J. Zhang, P. Zhong, Controllable synthesis of brookite/anatase/rutile TiO2 nanocomposites and single-crystalline rutile nanorods array, J. Mater. Chem. 22 (16) (2012) 7937–7944.

[21] E. Hendry, M. Koeberg, B. O'Regan, M. Bonn, Local field effects on electron transport in nanostructured TiO2 revealed by terahertz spectroscopy, Nano Lett. 6 (4) (2006) 755–759.
[22] E. Hosono, S. Fujihara, K. Kakiuchi, H. Imai, Growth of submicrometer-scale rectangular parallelepiped rutile TiO 2 films in aqueous TiCl3 solutions under hydrothermal conditions, J. Am. Chem. Soc. 126 (25) (2004) 7790–7791.
[23] S.Y. Lee, S.J. Park, TiO2 photocatalyst for water treatment applications, J. Ind. Eng. Chem. 19 (6) (2013) 1761–1769.
[24] X. Zu, H. Wang, G. Yi, Z. Zhang, X. Jiang, J. Gong, H. Luo, Self-powered UV photodetector based on heterostructured TiO2 nanowire arrays and polyaniline nanoflower arrays, Synth. Met. 200 (2015) 58–65.
[25] S. Sadhu, A. Jaiswal, S. Adyanthaya, P. Poddar, Surface chemistry and growth mechanism of highly oriented, single crystalline TiO2 nanorods on transparent conducting oxide coated glass substrates, RSC Adv. 3 (6) (2013) 1933–1940.
[26] M.R. Usman, A.R. Noviyanti, D.R. Eddy, The role of base solvent variant to structure and crystal size titanium dioxide by hydrothermal method, indones, J. Chem. 17 (1) (2017) 22.
[27] G.C. Collazzo, S.L. Jahn, E.L. Foletto, Temperature and reaction time effects on the structural properties of titanium dioxide nanopowders obtained via the hydrothermal method, Braz. J. Chem. Eng. 28 (2) (2011) 265–272.